IJIE

INTERNATIONAL JOURNAL OF INTEGRATED ENGINEERING
ISSN: 2229-838X e-ISSN: 2600-7916

Vol. 18 No. 2 (2026) 240-249
https://publisher.uthm.edu.my/ojs/index.php/ijie

Finite Element Analysis of Interface Pressure of Transtibial Residual Limb Using Conventional and 3D-Printed Prosthetic Socket During Gait Cycle

Hairul Bakri[1,2], Adila Fazliana Che Manan[1], Masjuri Musa[1,2], Mohd Nazim Abdul Rahman[1,2], Nguyen Ho Quang[3], Guo Dong Lim[4], Mohd Juzaila Abd Latif[1,2]*

[1] *Fakulti Teknologi dan Kejuruteraan Mekanikal,*
Universiti Teknikal Malaysia Melaka, Hang Tuah Jaya, 76100 Durian Tunggal, Melaka, MALAYSIA
[2] *Centre for Advanced Research on Energy (CARe),*
Universiti Teknikal Malaysia Melaka (UTeM), Hang Tuah Jaya, 76100 Durian Tunggal, Melaka, MALAYSIA
[3] *Institute of Engineering and Technology,*
Thu Dau Mot University, Thu Dau Mot City, Binh Duong Province, VIETNAM
[4] *Pusat Rehabilitasi PERKESO Sdn Bhd,*
Lot PT7263 Bandar Hijau, Hang Tuah Jaya, 75450 Melaka, MALAYSIA

*Corresponding Author: juzaila@utem.edu.my
DOI: https://doi.org/10.30880/ijie.2026.18.02.019

Article Info

Received: 3 November 2025
Accepted: 12 March 2026
Available online: 18 May 2026

Keywords

Transtibial prosthetic socket, gait cycle, finite element analysis, interface pressure

Abstract

This study examines the interface pressure distribution within transtibial prosthetic sockets during the gait cycle using finite element analysis (FEA) to improve comfort and load transfer for amputees. Discomfort caused by improper pressure distribution remains a major concern in prosthetic design, often leading to skin irritation, pain, and reduced mobility. To address this issue, the study compares conventional sockets with 3D-printed designs that offer enhanced customization and pressure relief. A validated FE model was developed to simulate the biomechanical interaction between the residual limb and prosthetic socket, incorporating anatomically relevant geometry and material properties. Interface pressures were analyzed at key points of interest, including the patella tendon, distal tibia end, fibula head, and popliteal regions, throughout the various phases of the gait cycle to capture dynamic pressure variations. Results indicate that 3D-printed sockets consistently demonstrate lower and more evenly distributed interface pressures than conventional sockets, with a maximum pressure reduction of 51.7% at the tibial end. The pressure values remained within established physiological limits throughout the gait cycle. The influence of knee flexion moments on pressure distribution was found to be minimal, suggesting that body weight and socket alignment are more critical factors. These findings support the application of 3D-printing technologies in prosthetic socket design to improve comfort, fit, and functionality for transtibial amputees.

1. Introduction

Transtibial amputation, a surgical procedure involving the removal of the lower limb below the knee, is often necessitated by diseases, accidents, injuries, trauma, or vascular complications [1], [2], [3]. This loss significantly alters an individual's mobility and quality of life, making effective prosthetic limbs essential for restoring functionality [4]. The socket serves as the pivotal interface for load transfer, comfort, and stability between the residual limb and prosthesis [5]. However, socket fit remains a persistent challenge, which is reported as the primary factor affecting rehabilitation by 48% of amputees and 65.7% of clinicians [6]. Poor fit can lead to discomfort, skin breakdown, biomechanical compensations, pressure sores, and pain, thereby discouraging the use of prostheses [7], [8].

Understanding pressure distribution at the residual limb-socket interface is essential for improving prosthetic socket comfort and minimizing the risk of tissue injury. Advances in sensor technology have enabled real-time measurement of interface pressure during activities such as walking [9]. These data support more informed socket design and fabrication, leading to reduced pressure on vulnerable anatomical regions [10]. Optimizing pressure distribution has been shown to enhance both the comfort and safety of prosthesis user outcomes [11], [12].

Finite element analysis (FEA) has become an important tool in evaluating the biomechanics of prosthetic sockets. It allows simulation of stress distribution and soft tissue deformation under various load conditions [13], [14], [15]. FEA supports the optimization of material use and geometry, particularly for modern manufacturing approaches such as 3D printing [16], [17]. This enables the development of patient-specific designs that balance between structural performance and user comfort.

Modern prosthetic interfaces have evolved, with improvements in socket designs, volume, and thermal control mechanisms, and the emergence of osseointegration [18]. Digital fabrication techniques, including CAD/CAM and additive manufacturing, are being explored to streamline production processes and enhance access to assistive technologies [19]. Despite these advances, many conventional sockets do not dynamically accommodate pressure variations during the gait cycle. Localized high-pressure areas, especially at the distal tibia, remain a common source of pain and dissatisfaction [20[, [21]. Rigid socket structures often fail to respond to the changing biomechanical demands of walking [5]. Addressing these issues requires a detailed analysis of pressure fluctuations throughout the gait cycle.

However, despite advances in prosthetic design, conventional sockets often fail to achieve optimal pressure distribution, leading to discomfort, skin complications, and reduced mobility in transtibial amputees. This study investigates the interface pressure distribution in transtibial prosthetic sockets using FEA, comparing conventional and 3D-printed designs across the gait cycle. By modeling mechanical interactions between the residual limb and socket under dynamic loading conditions, it aims to identify critical pressure points and structural weaknesses. The research seeks to inform the development of more responsive and comfortable socket designs. These findings may help improve mobility and quality of life for lower-limb amputees.

2. Methodology

2.1 Subject

The participant selected for this study was a 59-year-old male, with 162 cm height and 62 kg weight, who underwent a transtibial (below-knee) amputation of the right leg in February 2023 due to complications from Diabetes Mellitus (diabetic foot ulcer). The subject received rehabilitation treatment at Pusat Rehabilitasi PERKESO Sdn. Bhd. (PRPSB), Melaka. Ethical approvals for the study were obtained from PRPSB (PRPTAR/R&D/092021/0003) and Universiti Teknikal Malaysia Melaka (UTeM. 47.01.01/500-25/16-(13)).

2.2 Fabrication of Conventional Prosthetic Socket

The conventional prosthetic socket was fabricated by a certified prosthetist at PRPSB. The process included stump measurement, mould creation, rectification, and socket fabrication using the vacuum casting technique, as illustrated in Fig. 1. Each step was carefully conducted to ensure proper anatomical fit and alignment. This conventional approach served as a baseline for comparison with the digitally fabricated 3D-printed socket.

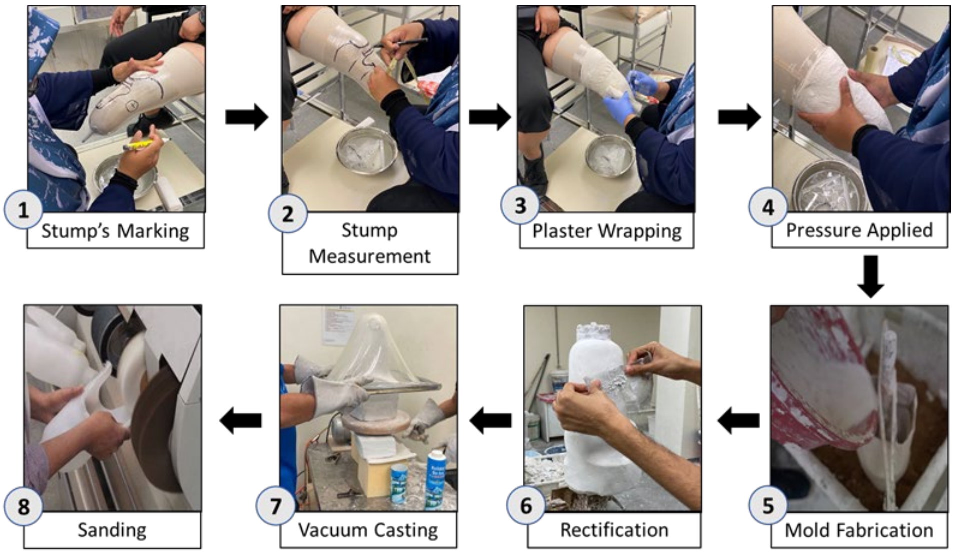

Fig. 1 *Conventional prosthetic socket fabrication process*

2.3 Fabrication of 3D-Printed Prosthetic Socket

The fabrication of the 3D-printed socket involved three main stages: 3D scanning of the stump, digital socket design, and 3D printing of the socket, as shown in Fig. 2. A full 360-degree scan of the residual limb was performed using the EinScan Pro 2X handheld scanner while the subject remained still. The captured mesh geometrical data was exported in STL format and imported into Fusion360 CAD software for digital rectification. A cylinder model was adapted to the residual limb, incorporating relief in pressure-sensitive regions and reinforcement in pressure-tolerant areas to enhance comfort and stability. The final socket design was printed using the Raise3D Pro2 Plus 3D printer with PLA filament. The printing parameters are summarized in Table 1.

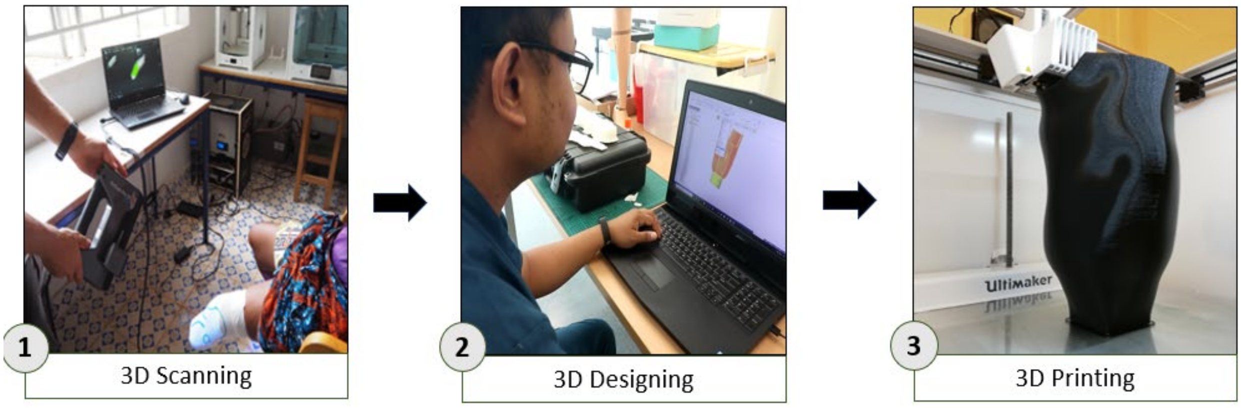

Fig. 2 *3D printed prosthetic socket fabrication process*

Table 1 *3D printing parameters*

Printing Parameter	Setting
Nozzle diameter (mm)	0.8
Layer thickness (mm)	0.4
Infill percentage (%)	100
Printing speed (mm/s)	50
Nozzle temperature (°C)	230
Bed temperature (°C)	60

During the rectification stage, adjustments were performed under the supervision of a prosthetist in PRPSB to ensure proper socket fit. In Fusion30, color-coded regions guided the modifications, where white indicated extruded zones (for reducing contact pressure in sensitive areas), and green/blue indicated indented zones (to increase contact force in pressure-tolerant areas), as illustrated in Fig. 3. These rectifications prevented bone contact in vulnerable zones while ensuring the socket remained secure during movement. This digital rectification approach offered enhanced control over load distribution compared to conventional methods.

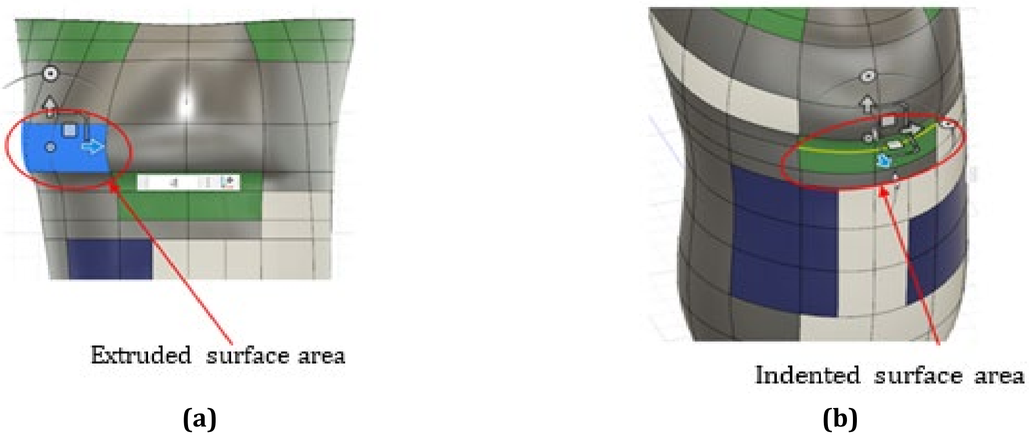

Fig. 3 *Socket design (a) Extrusion for pressure relief; (b) Indentation for targeted pressure application*

2.4 Development of Finite Element Model

2.4.1 Finite Element Model of Transtibial Prosthetic Assembly

The finite element (FE) model of the transtibial prosthetic was developed to simulate the biomechanical interaction between the socket, residual limb, and underlying knee joint bone. The geometric reconstruction of the residual limb and socket was achieved by importing STL files derived from 3D scanning into Fusion360 software. This process ensured precise anatomy, capturing the external contours and volumetric characteristics of the soft tissue.

To incorporate the skeletal structure, the knee joint was modelled based on MRI data acquired using the Esoate c-scan system, with a slice thickness of 2 mm and pixel size of 1 mm. Subsequently, segmentation of the distal femur and proximal tibial bone was performed within the Fusion360 environment. The segmented knee bone was anatomically positioned within the residual limb model, maintaining accurate spatial alignment. This integration enabled the construction of a comprehensive anatomical assembly that accurately represents the interface between the socket, soft tissue, and osseous structures of the knee joint, thereby facilitating detailed biomechanical analysis under various loading conditions. The completed transtibial prosthetic 3D model was then imported into ANSYS software to generate the FE mesh and conduct biomechanical simulations under physiological loading conditions, as shown in Fig. 4.

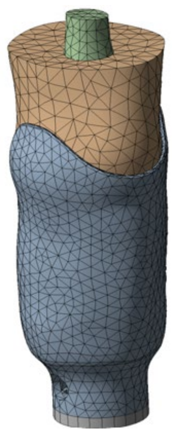

Fig. 4 *FE model of transtibial prosthetic*

2.4.2 Material Properties

The FE model consists of the socket-residual limb assembly, which was modelled as linear elastic, homogeneous, and isotropic materials to simplify the computational process while maintaining a reasonable degree of biomechanical accuracy. The material properties were selected based on values reported in the literature to reflect the mechanical behavior of each domain under physiological conditions.

The prosthetic socket, fabricated using polylactic acid (PLA), was assigned an elastic modulus of 2.64 GPa and a Poisson's ratio of 0.4, typical characteristics of high-density thermoplastics used in additive manufacturing. The soft tissue component, which encapsulates skin, muscle, ligaments, and other subcutaneous structures, was assigned a significantly lower elastic modulus of 60 KPa to reflect its compliant nature, along with a Poisson's ratio of 0.45 to account for its near-incompressibility. While for the knee joint bone was modelled as cortical bone with an elastic modulus of 30 GPa and a Poisson's ratio of 0.3, consistent with established biomechanical parameters for human femoral or tibial bone tissue. Additional mechanical properties such as density, bulk modulus, and shear modulus for each material domain are summarized in Table 2.

Table 2 *Material properties of the FE model [22]*

Property	PLA	Soft Tissue	Knee Joint Bone
Density (kg/m^3)	2000	1000	2000
Elastic Modulus (Pa)	2.64×10^9	60×10^3	30×10^9
Poisson's ratio	0.4	0.45	0.3
Bulk Modulus (Pa)	4.39×10^9	200×10^3	25×10^9
Shear Modulus (Pa)	0.94×10^9	20.69×10^3	11.54 10^9

2.4.3 Boundary and Loading Conditions

The interface between the 3D-printed socket and residual stump was defined as frictional contact with a coefficient of 0.5, while the interface between the knee joint bone and residual limb soft tissue was modelled as bonded contact [22]. For FE model validation, the initial loading was applied in the static standing position using half-body weight. Dynamic loading was simulated for five phases of the gait cycle during heel strike, loading response, midstance, terminal stance, and pre-swing. Single-support phases (loading response, midstance, terminal stance) received full-body weight, while double-support phases (heel strike and pre-swing) received half-body weight. Knee flexion moments were also applied based on corresponding hip flexion angles during the gait cycle, with the femur length set at 0.45 m. The loading conditions are summarized in Table 3.

Table 3 *Loading conditions for FEA during gait cycle [23]*

Gait Phase	Hip Flexion Angle (°)	Knee Flexion Angle (°)	Support Type
Heel strike	25	10	Double
Loading response	18	15	Single
Midstance	5	5	Single
Terminal stance	-10	0	Single
Pre-swing	-20	15	Double

3. Results

3.1 Validation of Finite Element Model

Table 4 presents a comparison between the experimental measurements and FEA results for interface pressure distribution at key points of interest (POIs) on the residual limb-socket of a 3D-printed transtibial prosthetic socket. The results demonstrate strong agreement between the FEA predictions and the experimental data, with percentage errors ranging from 2.0% to 14.4%. This agreement indicates the reliability of the developed FE model, where the assigned material properties, boundary conditions, and contact definitions within the FE framework were sufficient to replicate the biomechanical interaction at these critical load-bearing sites.

Table 4 *Comparison of interface pressure distribution between experimental and FE results of 3D-printed socket*

Area	Point of Interest	Interface Pressure (kPa)		Percentage Error (%)
		Experiment	FEA	
Middle	Patella Tendon	27.44	27.98	2.0
Distal	Tibia End	32.79	28.79	12.2
Middle	Medial Middle	20.65	23.63	14.4
Proximal	Popliteal	26.49	25.85	2.4

The patella tendon and popliteal regions show excellent agreement, with percentage errors of only 2.0% and 2.4%, respectively. This suggests that the FE model accurately captures the mechanical interaction between the socket and the residual limb in these regions. In contrast, the medial middle and tibia end exhibit slightly higher errors of 14.4% and 12.2%, respectively. These deviations can be attributed primarily to the simplification in the residual limb model, particularly the exclusion of detailed anatomical segmentation such as muscle, ligament, and skin layers, which may influence local tissue deformation under load.

The overall validation confirms that the FE model effectively captures the fundamental mechanics of pressure transfer between the stump and socket, making it suitable for subsequent biomechanical investigations. The observed discrepancies, although modest, highlight the inherent challenges of representing the heterogeneous and nonlinear properties of biological tissues in computational models. Previous studies have similarly reported that uniform assignment of soft tissue properties can lead to slight overestimations in pressure magnitudes at localized regions of high stiffness [24, 25]. Despite these limitations, the present model successfully predicts pressure magnitudes and trends across all POIs, thereby supporting its utility as a reliable tool for comparative assessments between different socket designs.

3.2 Comparison of Interface Pressure Distribution Between Conventional and 3D-Printed Sockets

A comparative FEA of interface pressure distribution demonstrates distinct differences between conventional and 3D-printed transtibial prosthetic sockets. As shown in Table 5, the 3D-printed socket consistently exhibits reduced interface pressure across all POIs relative to the conventional socket. This reduction is most pronounced at the tibia end, where the pressure drops from 67.82 kPa in the conventional socket to 32.79 kPa in the 3D-printed design, representing a 51.7% decrease. Such reductions suggest that the 3D-printed socket more effectively distributes loads in pressure-sensitive regions, thereby minimizing discomfort and risk of soft tissue injury.

Table 5 *Comparison of interface pressure distribution between experimental and FE results of 3D-printed socket*

Area	Point of Interest	Interface Pressure (kPa)		Percentage Difference (%)
		Conventional Socket	3D-Printed Socket	
Middle	Patella Tendon	43.55	27.44	37.0
Distal	Tibia End	67.82	32.79	51.7
Middle	Medial Middle	34.62	20.65	40.4
Proximal	Popliteal	33.10	26.49	20.0

Similarly, the patella tendon area exhibits a 37.0% reduction in interface pressure, declining from 43.55 kPa to 27.44 kPa. This outcome is particularly important, as the patella tendon is a pressure-tolerant zone, and maintaining optimal load transfer here is essential for both function and comfort. The 3D-printed socket appears to support a more biomechanically favourable alignment, thereby mitigating the risk of excessive localized stress. Additionally, the medial middle and popliteal regions experience pressure reductions of 40.4% and 20.0%, respectively, further emphasizing the advantages of 3D-printed geometries in improving fit and interface stress distribution.

The ability to reduce interface pressure at these anatomical sites is attributed to the superior adaptability and design freedom afforded by 3D printing. Unlike conventional socket fabrication methods, which often rely on manual casting and iterative adjustments, additive manufacturing enables precise anatomical conformity and controlled material distribution. This allows for the deliberate redistribution of pressure toward load-bearing

Int. Journal of Integrated Engineering Vol. 18 No. 2 (2026) p. 240-249

areas while alleviating stress in sensitive zones. Consequently, amputees may experience enhanced comfort, better suspension, and longer wear time due to decreased tissue strain and reduced risk of pressure sores.

These findings align closely with prior studies, including those by Tang et al. [24], who demonstrated that personalized 3D-printed sockets significantly improve pressure distribution and gait performance. Moreover, conventional sockets often fail to accommodate residual limb volume fluctuations and asymmetries, resulting in uneven load transfer and discomfort over extended use [26]. Amputees have reported challenges in wearing such sockets continuously, largely due to the rigidity and lack of dynamic fit adjustment [27]. By contrast, 3D-printed sockets offer a patient-specific approach that has the potential to transform clinical prosthetics by combining digital precision with biomechanical optimization.

3.3 Interface Pressure Distribution Across Gait Phases

3.3.1 Anterior-Posterior Pressure Distribution

Fig. 5 illustrates the dynamic variation of interface pressure at three key POIs, which are the patella tendon, tibia end, and popliteal during different phases of the gait cycle. The patella tendon region demonstrates a relatively consistent pressure profile throughout most of the cycle, with a prominent peak of 51.57 kPa during midstance. This spike in pressure is attributed to the full body weight acting vertically on the limb during midstance, in the absence of significant rotational effects caused by hip flexion. In phases such as heel strike and loading response, the hip flexion moment introduces a counteracting anticlockwise rotation (with relative hip-knee angles of 15° and 3°, respectively), which offsets some of the vertical load and results in lower interface pressures.

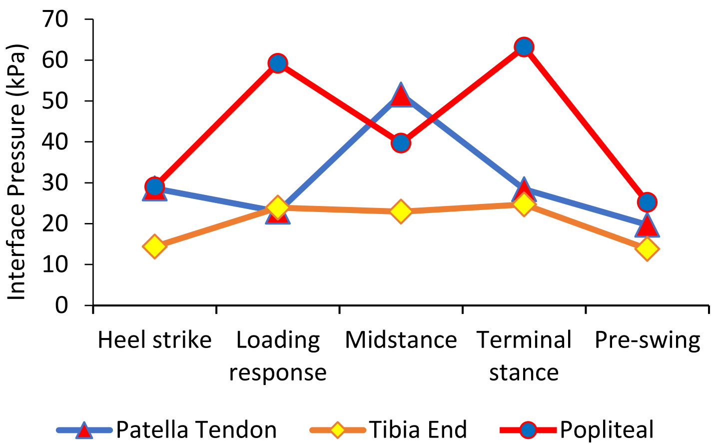

Fig. 5 *Interface pressure at the anterior-posterior of 3D-printed socket across the gait cycle*

The interplay between residual limb movement and socket mechanics plays a crucial role in pressure variation. During terminal stance and pre-swing, the flexion dynamics of the hip similarly act to moderate the load, producing lower and more stable interface pressures. These phases are characterized by reduced vertical force transfer due to limb propulsion and body weight shift toward the contralateral limb. Hence, the pressure behavior at the patella tendon is largely governed by the balance of vertical load and flexion-induced displacement, with peak loading occurring during midstance when the body's center of mass is directly above the limb.

In contrast, the tibia end region consistently experiences the lowest interface pressures, fluctuating between 20 kPa and 30 kPa throughout the gait cycle. The minimal variation in pressure at this location suggests effective load distribution and cushioning provided by the socket design, especially in a pressure-intolerant region like the tibial end. The relatively flat pressure profile indicates this region is less sensitive to gait dynamics, affirming the biomechanical design's success in minimizing stress concentration. This outcome is significant, as high pressure at the tibia end can lead to discomfort and soft tissue damage, particularly in amputees with limited residual limb padding.

The popliteal area, however, shows a markedly different trend, with pressure readings peaking at 65 kPa and 70 kPa during midstance and terminal stance. This double-hump pattern corresponds with the phases of highest load transfer, in agreement with findings by Sengeh and Herr [28] and Devin et al. [24]. These peaks reflect moments of maximal body weight support and forward propulsion, which subject the posterior socket region to intense localized forces. The magnitude of pressure at the popliteal fossa highlights the need for careful socket contouring and material selection in this anatomically sensitive region to reduce discomfort and prevent circulatory issues.

3.3.2 Medial-Lateral Pressure Distribution

The medial-lateral interface pressure behaviour, depicted in Fig. 6, reveals distinct dynamic profiles for the medial middle and fibula head during the gait cycle. Both regions exhibit a characteristic double-hump curve, with pressure increases during loading response and terminal stance, and a drop during midstance. At the medial middle, peak interface pressures of 43.60 kPa and 44.08 kPa are recorded during loading response and terminal stance, respectively, while a lower pressure of 24.07 kPa is observed in midstance. The trend of the result agrees with Nandikolla et al. [29], where this fluctuation aligns with the body's transition from double to single limb support, during which pressure is concentrated on one limb, causing increased socket-limb interaction forces.

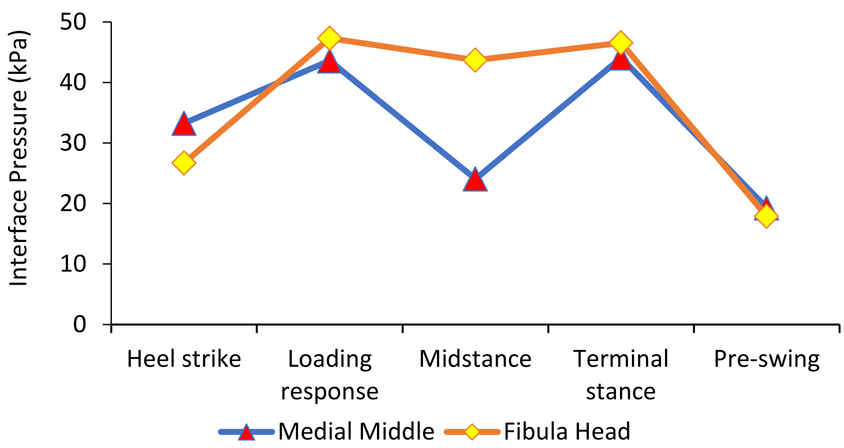

Fig. 6 *Interface pressure at the medial-lateral of 3D-printed socket across the gait cycle*

The single support phases, which include loading response, midstance, and terminal stance, account for approximately 60% of the gait cycle. During these periods, all ground reaction forces are borne by the prosthetic limb, intensifying the pressure at the residual limb-socket interface. The observed pressure trends at the medial middle are consistent with mechanical expectations, whereby weight shifts result in lateral compression as the socket stabilizes the limb against medial-lateral movement. This suggests that targeted support and accommodation are essential in the medial middle region to manage fluctuating interface loads.

The fibula head region, representing the lateral aspect of the residual limb, shows even higher interface pressures during the same phases. Recorded pressures are 47.32 kPa during loading response, 43.71 kPa during midstance, and 46.57 kPa during terminal stance. These elevated values highlight the structural prominence and limited soft tissue padding over the fibular head, which leads to increased susceptibility to pressure peaks. The fibular region appears to experience more uneven loading, likely due to socket rigidity and the asymmetric geometry of the residual limb, necessitating special attention during socket design and fitting.

Additionally, the pressure trend in the pre-swing phase is consistently lower compared to heel strike across both medial and lateral regions. This is attributed to the offloading of body weight as the limb prepares to enter the swing phase, leading to reduced vertical forces and diminished socket-stump interaction. During heel strike, however, a sudden flexion of the knee occurs to absorb the impact, resulting in a brief surge of pressure, especially in lateral structures. These insights underscore the dynamic and region-specific loading patterns experienced during ambulation, reaffirming the importance of designing sockets that adapt to the biomechanical demands of each gait phase.

4. Conclusion

The present study demonstrated that FEA is an effective tool for evaluating interface pressure distribution between the residual limb and prosthetic socket in transtibial amputees. Validation against experimental data confirmed the accuracy of the FEA model, particularly at critical anatomical points. Comparative analysis showed that 3D-printed sockets consistently reduced interface pressure across all points of interest compared to conventional sockets, with the greatest reduction of 51.7% observed at the tibial end. These reductions indicate improved pressure distribution and potential for enhanced user comfort and mobility. The findings underscore the clinical relevance of 3D-printed, anatomically optimized sockets and support their continued development as a viable alternative to conventional prosthetic designs.

Acknowledgement

This research is funded by Malaysian Technical University Network (MTUN) grant (Industri (MTUN)/PRPSB/2020/FKM-CARE/100047). The support from Universiti Teknikal Malaysia Melaka (UTeM) is gratefully acknowledged.

Conflict of Interest

Authors declare that there is no conflict of interests regarding the publication of the paper.

Author Contribution

*The authors confirm contribution to the paper as follows: **conventional and 3D-printed socket fabrication**: H.B, A.F.C.M, G.D.L; **FE model development and simulation**: H.B, M.M, M.N.AR, N.H.Q, M.J.A.L.; **data collection**: H.B, A.F.C.M, M.J.A.L.; **analysis and interpretation of results**: H.B, A.F.C.M, M.J.A.L.; **draft and manuscript preparation**: H.B, M.J.A.L. All authors reviewed the results and approved the final version of the manuscript.*

References

[1] Davie-Smith, F., Coulter, E., Kennon, B., Wyke, S., & Paul, L. (2017). Factors influencing quality of life following lower limb amputation for peripheral arterial occlusive disease: A systematic review of the literature. *Prosthetics and Orthotics International, 41*(6), 537–547. https://doi.org/10.1177/0309364617690394

[2] Beckman, J. A., Duncan, M. S., Damrauer, S. M., Wells, Q. S., Barnett, J. V., Wasserman, D. H., & Bedimo, R. J. (2019). Microvascular disease, peripheral artery disease, and amputation. *Circulation, 140*(6), 449–458. https://doi.org/10.1161/CIRCULATIONAHA.119.040672

[3] Irawan, A. P., Utama, D. W., Setiawan, A. S., Laksmidewi, D., Fitriyana, D. F., Wicaksana, Y. S., & Priyani P.A., Anis, A., Cionita, T., Siregar, J.P., Jaafar, J., Manalu, J., & Numberi, J.J. (2024). An overview of the below knee prosthesis socket fabrication made from natural fiber composite. *International Journal of Integrated Engineering, 16*(9), 190-208. https://doi.org/10.30880/ijie.2024.16.09.015

[4] Alluhydan, K., Siddiqui, M. I. H., & Elkanani, H. (2023). Functionality and comfort design of lower-limb Ansprosthetics: A review. *Journal of Disability Research, 2*(3), 10–23. https://doi.org/10.57197/JDR-2023-0031

[5] Wang, M., Nong, Q., Liu, Y., & Yu, H. (2022). Design of lower limb prosthetic sockets: A review. *Expert Review of Medical Devices, 19*(1), 63–73. https://doi.org/10.1080/17434440.2022.2020094

[6] Turner, S., & McGregor, A. H. (2020). Perceived impact of socket fit on major lower limb prosthetic rehabilitation: A clinician and amputee perspective. *Archives of Rehabilitation Research and Clinical Translation, 2*(3), 100059. https://doi.org/10.1016/j.arrct.2020.100059

[7] Finco, M. G. (2022). Musculoskeletal and biomechanical adaptations post amputation. *The FASEB Journal, 36*(S1), 0I608. https://doi.org/10.1096/fasebj.2022.36.S1.0I608

[8] Knight, A. D., Dearth, C. L., & Hendershot, B. D. (2021). Deleterious musculoskeletal conditions secondary to lower limb loss: Considerations for prosthesis-related factors. *Advances in Wound Care, 10*(12), 671–684. https://doi.org/10.1089/wound.2019.1079

[9] Tang, J., Liu, X., Liu, Z., & Li, W. (2023). Optimal design and 3D printing of prosthetic socket based on the interface pressure between the socket and residual limb. *Prosthetics & Orthotics International, 47*(1), 87–93. https://doi.org/10.1097/PXR.0000000000000147

[10] Lee, S., Kwon, H., Jung, S. Y., Shin, H. J., Kwon, C. Y., & Kim, J. H. (2021). Pressures monitored by 3D printed capacitive pressure sensor embedded on prosthetic upper limb socket: A case study. *Journal of Biomechanical Science and Engineering, 16*(3), 2100077. https://doi.org/10.1299/jbse.21-00077

[11] Armitage, L., Buller, A., Rajan, G., Prusty, G., Simmons, A., & Kark, L. (2020). Clinical utility of pressure feedback to socket design and fabrication. *Prosthetics and Orthotics International, 44*(1), 18–26. https://doi.org/10.1177/0309364619868364

[12] Abbod, E. A., & Resan, K. K. (2021). Review on the interface pressure measurement for below knee prosthetic socket. *IOP Conference Series: Materials Science and Engineering, 1094*(1), 012036. https://doi.org/10.1088/1757-899X/1094/1/012036

[13] Singh, J. J., Mehta, J. S., Kumar, R., & Sapra, G. (2022). FEA simulations of lower limb prosthetics. *IOP Conference Series: Materials Science and Engineering, 1225*(1), 012030. https://doi.org/10.1088/1757-899X/1225/1/012030

[14] Steer, J. W., Worsley, P. R., Browne, M., & Dickinson, A. S. (2020). Predictive prosthetic socket design: Part 1—Population based evaluation of transtibial prosthetic sockets by FEA driven surrogate modelling. *Biomechanics and Modeling in Mechanobiology, 19*(4), 1331–1346. https://doi.org/10.1007/s10237-019-01195-5

[15] Baharuddin, M.H., Ab Rashid, A.M., Azrin Abullah, N.N.A., Ramlee, M.H. (2024). Patient-specific design of prosthesis for below kne amputee: analysis between different gait. *International Journal of Integrated Engineering, 16*(5), 214-223. https://doi.org/10.30880/ijie.2024.16.05.017

[16] Mohamed Norli, M. H., Abdullah, A. H., Sukimi, A. K. A., Mahmud, J., & Ramlee, M. H. (2024). Static structural analysis on different topology optimization transtibial prosthetic socket leg. *International Journal of Technology, 15*(2), 455–462. https://doi.org/10.14716/ijtech.v15i2.6711

[17] Jindal, P., Prakash, P., Bassal, H., Singh, P., Din, M. A. M., Barnett, C. T., & Breedon, P. (2025). Two material-based transtibial socket designs for enhanced load bearing capacity using FEA. *Prosthesis, 7*(2), Article 30. https://doi.org/10.3390/prosthesis7020030

[18] Safari, R. (2020). Lower limb prosthetic interfaces: Clinical and technological advancement and potential future direction. *Prosthetics and Orthotics International, 44*(6), 384–401. https://doi.org/10.1177/0309364620969226

[19] Oldfrey, B. M., Morgado Ramirez, D. Z., Miodownik, M., Wassall, M., Ramstrand, N., Wong, M. S., Danemayer, J., Dickinson, A., Kenney, L., Nester, C., Lemaire, E., Gholizadeth, H., Diment, L. E., Donovan-Hall, M. K., & Holloway, C. (2024). A scoping review of digital fabrication techniques applied to prosthetics and orthotics: Part 1 of 2—Prosthetics. Prosthetics and Orthotics International, 48(5), 574–589. https://doi.org/10.1097/PXR.0000000000000126

[20] Lee, P. S., Gao, R. Z., Colpitts, A., Murdock, R. W., Dittmer, D., Schirm, A., Tung, J. Y., & Ren, C. L. (2022). Air microfluidics enabled soft robotic transtibial prosthesis socket liner toward dynamic management of residual limb contact pressure and volume fluctuation. *Biomicrofluidics, 16*(3), 034107. https://doi.org/10.1063/5.0087900

[21] Hsu, C. H., Ou, C. H., Hong, W. L., & Gao, Y. H. (2018). Comfort level discussion for prosthetic sockets with different fabricating processing conditions. *BioMedical Engineering Online, 17*(Suppl. 2), 145. https://doi.org/10.1186/s12938-018-0577-2

[22] Dickinson, A. S., Steer, J. W., & Worsley, P. R. (2017). Finite element analysis of the amputated lower limb: A systematic review and recommendations. *Medical Engineering & Physics, 43*, 1–18. https://doi.org/10.1016/j.medengphy.2017.02.008

[23] Villarreal, D. J., Embry, K. R., & Gregg, R. D. (2017). A robust parameterization of human gait patterns across phase shifting perturbations. *IEEE Transactions on Neural Systems and Rehabilitation Engineering, 25*(3), 265–278. https://doi.org/10.1109/TNSRE.2016.2569019

[24] Tang, J., Liu, X., Liu, Z., & Li, W. (2022). Optimal design and 3D printing of prosthetic socket based on the interface pressure between the socket and residual limb. *Prosthetics and Orthotics International, 47*(1), 87–93. https://doi.org/10.1097/PXR.0000000000000147

[25] Devin, K. M., Tang, J., Moser, D., & Jiang, L. (2023). Assessing socket fit effects on pressure and shear at a transtibial residuum/socket interface. *Applied Bionics and Biomechanics, 2023*, Article 3257059. https://doi.org/10.1155/2023/3257059

[26] Wang, M., Nong, Q., Liu, Y., & Yu, H. (2021). Design of lower limb prosthetic sockets: A review. *Expert Review of Medical Devices, 19*(1), 63–73. https://doi.org/10.1080/17434440.2022.2020094

[27] Turner, S., Belsi, A., & McGregor, A. H. (2021). Issues faced by people with amputation(s) during lower limb prosthetic rehabilitation: A thematic analysis. *Prosthetics and Orthotics International, 46*(1), 61–67. https://doi.org/10.1097/PXR.0000000000000070

[28] Sengeh, D. M., & Herr, H. (2013). A variable impedance prosthetic socket for a transtibial amputee designed from magnetic resonance imaging data. *Journal of Prosthetics and Orthotics, 25*(3), 129–137. https://doi.org/10.1097/JPO.0b013e31829be19c

[29] Nandikolla, V. K., Bochen, R., Meza, S., & Garcia, A. (2017). Experimental gait analysis to study stress distribution of the human foot. *Journal of Medical Engineering, 2017*, Article 3432074. https://doi.org/10.1155/2017/3432074